

LETTERS

Hybrid organic–inorganic rotaxanes and molecular shuttles

Chin-Fa Lee¹, David A. Leigh¹, Robin G. Pritchard², David Schultz¹, Simon J. Teat³, Grigore A. Timco² & Richard E. P. Winpenny²

The tetravalency of carbon and its ability to form covalent bonds with itself and other elements enables large organic molecules with complex structures, functions and dynamics to be constructed. The varied electronic configurations and bonding patterns of inorganic elements, on the other hand, can impart diverse electronic, magnetic, catalytic and other useful properties to molecular-level structures. Some hybrid organic–inorganic materials that combine features of both chemistries have been developed, most notably metal–organic frameworks¹, dense and extended organic–inorganic frameworks² and coordination polymers³. Metal ions have also been incorporated into molecules that contain interlocked subunits, such as rotaxanes^{4–7} and catenanes^{6,8}, and structures in which many inorganic clusters encircle polymer chains have been described⁹. Here we report the synthesis of a series of discrete rotaxane molecules in which inorganic and organic structural units are linked together mechanically at the molecular level. Structural units (dialkylammonium groups) in dumb-bell-shaped organic molecules template the assembly of essentially inorganic ‘rings’ about ‘axles’ to form rotaxanes consisting of various numbers of rings and axles. One of the rotaxanes behaves as a ‘molecular shuttle’¹⁰: the ring moves between two binding sites on the axle in a large-amplitude motion typical of some synthetic molecular machine systems^{11–15}. The architecture of the rotaxanes ensures that the electronic, magnetic and paramagnetic characteristics of the inorganic rings—properties that could make them suitable as qubits for quantum computers^{16–18}—can influence, and potentially be influenced by, the organic portion of the molecule.

The basis for the hybrid organic–inorganic rotaxane synthesis lies in the observation¹⁹ that the formation of heterometallic rings of various shapes and sizes, containing seven or more trivalent Cr(III) ions and one or two divalent metal ions (typically Ni(II), Co(II), Fe(II) or Cu(II)) bridged by multiple fluoride and alkyl/aryl carboxylate anions, is templated by various organic cations²⁰, including imidazolium²¹, *N*-alkylimidazolium²¹ and primary²² and secondary¹⁹ ammonium groups. Dialkylammonium salts have previously been used to direct the assembly of rotaxanes based on crown ethers^{23,24}, cucurbituril^{25,26} and cyclic peptides²⁷, so it seemed possible that they could also template the formation of rotaxanes using heterometallic rings. Secondary amine threads (1a–c) were constructed with bulky ‘stoppers’ at each end of the axle to prevent subsequent de-threading of the heterometallic ring assembled around the ammonium template. The threads were reacted¹⁹ with a 7:1 molar ratio of Cr(III):Co(II) ions in the form of chromium(III) fluoride (CrF₃·4H₂O) and a cobalt(II) pivalate salt ([Co₂(H₂O)(*t*-BuCO₂)₄(*t*-BuCO₂H)₄]; *t*-Bu, tert-butyl), with pivalic acid as the solvent, at 140 °C for 12 h (Fig. 1a). Although no rotaxane was observed with the shorter threads (1a and 1b), probably owing to there being insufficient space between the stoppers

to accommodate the bulky heterometallic ring, we found that with a six-carbon-atom spacer between the ammonium centre and each stopper (thread 1c), [2]rotaxane 2c was produced in 23% yield, which is rather efficient for what is essentially a 33-component assembly process (each metal–ligand bond is dynamic under the reaction conditions).

Confirmation of the interlocked nature of 2c was provided by the solid-state structure of a single crystal of the [2]rotaxane grown from a saturated diethyl ether/acetonitrile solution (Fig. 1b). The [2]rotaxane is a neutral molecule, the positive charge on the ammonium thread being balanced by the charge remaining on a heterometallic macrocycle consisting of 24 monoanionic ligands (eight fluorides and sixteen pivalate groups) bound to seven trivalent cations (Cr(III)) and one divalent (Co(II)) cation. The crystal structure shows the ammonium cation in the centre of the cavity of the macrocycle, forming short (~2.0 Å) F⁻···HN⁺ hydrogen bonds with two of the bridging fluoride ligands. Mass spectrometry confirms that each rotaxane molecule contains exactly one cobalt and seven chromium ions (Supplementary Information), the crystallographic data indicating that the cobalt ion is disordered over the eight different metal sites in each ring in the solid state (¹H NMR suggests that it also has no particularly favoured position in solution (see below)).

The X-ray structure shows the eight metal centres in each heterometallic wheel to be almost perfectly coplanar, with the two faces of the ring almost identical in terms of physical shape and geometry. Nevertheless, the wheel is intrinsically chiral (that is, has a non-superimposable mirror image) because the one Co(II) ion must have either a (Δ) arrangement or a (Λ) arrangement of the ligands in its octahedral coordination sphere (see Supplementary Information for an explanation of this nomenclature). The chirality is particularly apparent in the unequal magnetic effect exerted on each geminal proton in the methylene groups of the thread as revealed by ¹H NMR spectroscopy (see below). The sixteen pivalate groups form a lipophilic outer coating for the heterometallic ring, conferring good solubility of the rotaxane in a range of organic solvents, including toluene, dichloromethane, chloroform and diethyl ether.

Comparison of the ¹H NMR spectrum of the parent thread, 1c (Fig. 2a), with that of the rotaxane, 2c (Fig. 2b), and a partially deuterated analogue, d₁₄₄-2c (Fig. 2c, d), shows that the basic structure found in the solid state is retained in C₂D₂Cl₄ solution and also gives some information regarding the dynamics of the relative motion of the mechanically interlocked components. As one of the eight metal ions (Co(II)) is different from the other seven (Cr(III)) in each ring, if the heterometallic ring spun about the axis of the thread rapidly on the NMR timescale then the sixteen pivalate groups should experience eight non-equivalent sets of chemical environments—four for axial and four for equatorial pivalate groups—as observed

¹School of Chemistry, University of Edinburgh, The King's Buildings, West Mains Road, Edinburgh EH9 3JJ, UK. ²School of Chemistry, University of Manchester, Oxford Road, Manchester M13 9PL, UK. ³Advanced Light Source, Lawrence Berkeley Laboratory, 1 Cyclotron Road, MS2-400, Berkeley, California 94720, USA.

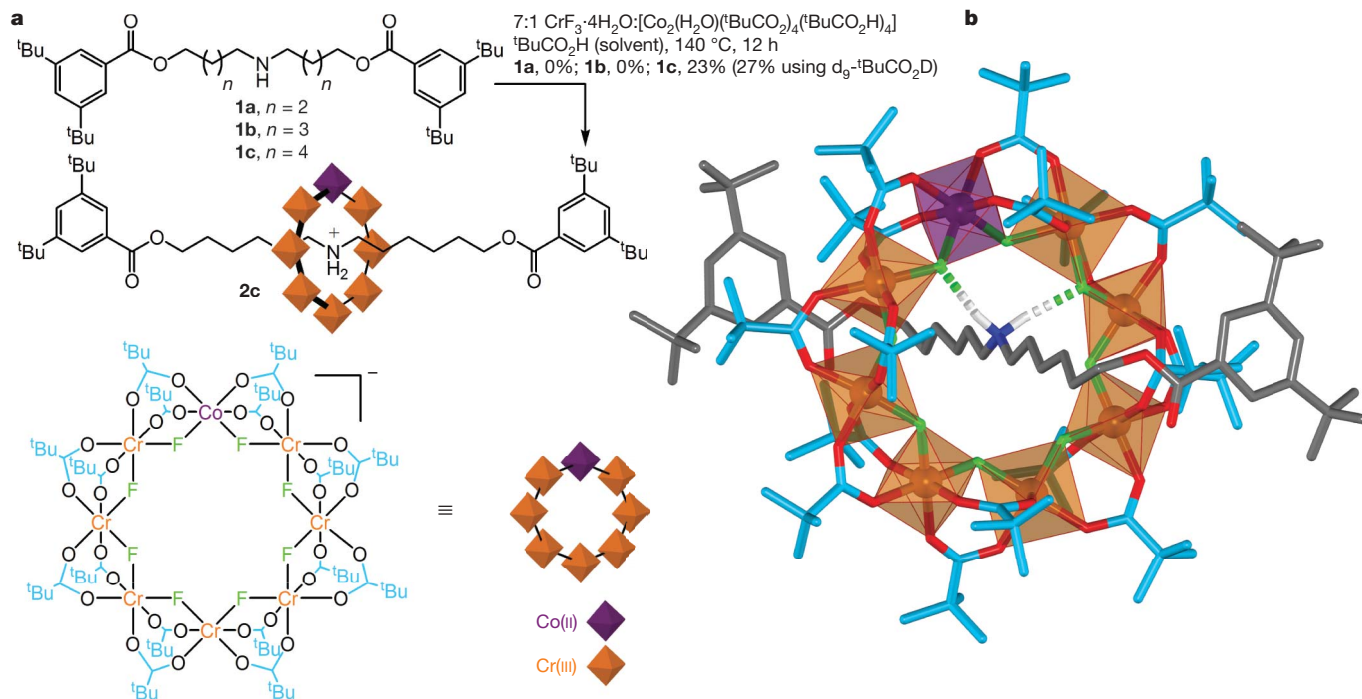


Figure 1 | Synthesis and X-ray crystal structure of hybrid organic-inorganic [2]rotaxane **2c.** **a**, Synthesis. ^tBu, tert-butyl. **b**, X-ray crystal structure. In the framework representation of the X-ray crystal structure, carbon atoms of the thread are shown in grey, those of the pivalate groups in light blue, oxygen atoms in red, nitrogen in dark blue, fluorine in green, cobalt in purple and chromium in orange. Hydrogen atoms (white) other than those of the ammonium group are omitted for clarity. The Co(II) ion is disordered over the eight metal sites in each heterometallic wheel. Both enantiomers, (Δ) or (Λ) at the Co(II) ion, are present in the crystal. Hydrogen-bond lengths and N-H-F angles are NH1···F1 = 2.03 Å, NH2···F7 = 2.01 Å, N-H1-

F1 = 168.9° and N-H2-F7 = 168.2°, shown as dashed cylinders in the figure. The fluorine anion between the two involved in short NH···F hydrogen bonds is also close enough to both ammonium protons to provide some electrostatic stabilization of the intercomponent binding motif (that is, it participates in what can be considered long and poorly directional NH···F hydrogen bonds, not depicted in the figure): NH1···F8 = 2.38 Å, NH2···F8 = 2.56 Å, N-H1-F8 = 114.2°, N-H2-F8 = 101.7°. Crystallographic data and experimental details of the structural refinement for **2c** are provided in the Supplementary Information.

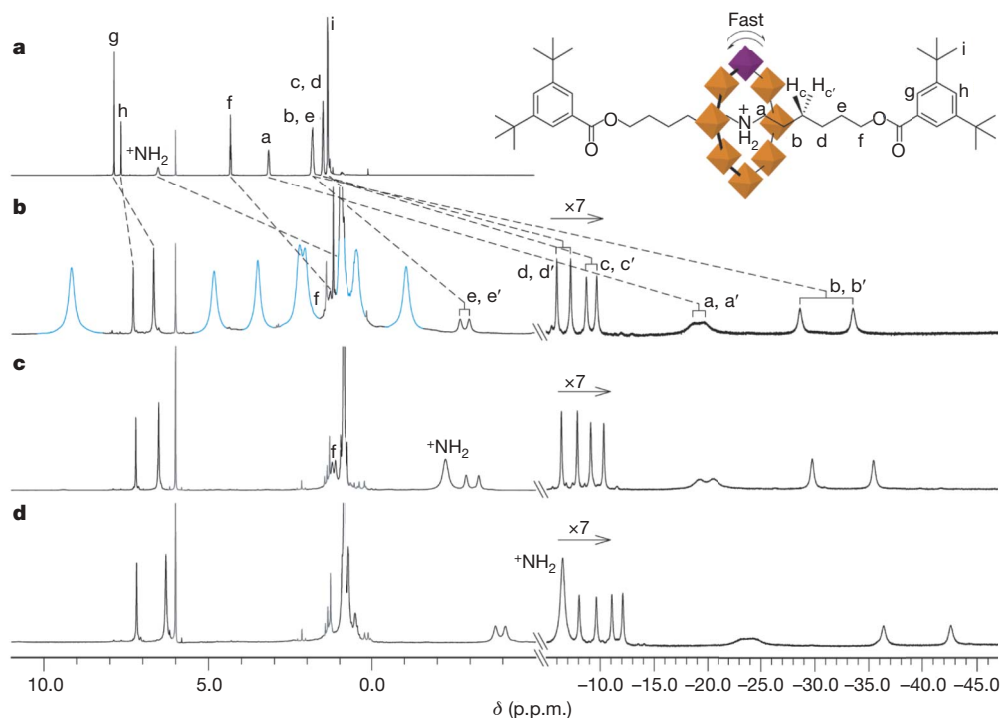


Figure 2 | ¹H NMR spectra (500 MHz, C₂D₂Cl₄). **a**, Thread **1c**·PF₆⁻ at 330 K. **b**, [2]rotaxane **2c** at 330 K. **c**, d₁₄₄-**2c** at 330 K. **d**, d₁₄₄-**2c** at 300 K. δ , chemical shift. The eight signals shown in blue in **b** are due to the 48 pivalate methyl groups of the macrocycle (see text and Supplementary Information for an explanation of the splitting pattern). Per-deuterating the pivalate

methyl groups facilitates characterization of the relatively low-intensity thread protons in the rotaxane (**c** and **d**). The rotaxane signals below -5 p.p.m. are shown at $\times 7$ magnification and on a compressed chemical-shift axis in comparison with the signals above -5 p.p.m. Residual solvent peaks and impurities are shown in grey.

for the parent macrocycle $[\text{Cr}_7\text{CoF}_8(t\text{-BuCO}_2)_{16}\cdot\text{H}_3\text{O}]$ (Supplementary Information). If, on the other hand, the ring were rotating slowly about the thread then it would become desymmetrized on the NMR timescale and many more non-equivalent sets of signals for the pivalate groups would be expected. Eight resonances for pivalate methyl groups (blue signals, Fig. 2b) are present for the [2]rotaxane at 330 K in $\text{C}_2\text{D}_2\text{Cl}_4$ (500 MHz), and as cooling to 240 K does not change this number, nor appreciably broaden the signals, it appears that the heterometallic ring rotates about the thread (randomly under thermal motion) very rapidly under these conditions.

The most dramatic effects of interlocking the inorganic and organic components, however, are the very large shifts (up to 45 p.p.m.; Fig. 2d) in the thread protons caused by the paramagnetic $\text{Co}(\text{II})$ ion, the greatest shifts generally occurring for the protons closest to the heterometallic wheel. The presence of two signals for each pair of methylene protons is due to the two protons of each methylene group (labelled primed and unprimed in Fig. 2) being diastereotopic (that is, magnetically distinct) given the chirality of the heterometallic wheel. The magnitude of the shifts is highly sensitive to changes in temperature (for example, there is a 6–8-p.p.m. change in the chemical shift of H_b and H_b' over a range of just 30 K; compare Fig. 2c with Fig. 2d).

The hybrid organic–inorganic rotaxane synthesis was successfully extended to threads containing more than one ammonium binding site (Fig. 3). This enabled the preparation of significantly more complex architectures (Fig. 4), including multi-ring [3]- and [4]rotaxanes and dynamic molecular shuttles in which the ring moves randomly under thermal motion between different binding sites on the thread.

With a long (12-carbon-atom) spacer between two ammonium groups on the thread (3b), reaction under the previously established conditions (7:1 $\text{CrF}_3\cdot 4\text{H}_2\text{O}:[\text{Co}_2(\text{H}_2\text{O})(t\text{-BuCO}_2)_4(t\text{-BuCO}_2\text{H})_4]$, $t\text{-BuCO}_2\text{H}$, 140 °C, 12 h) afforded [3]rotaxane 5b in 45% yield (from

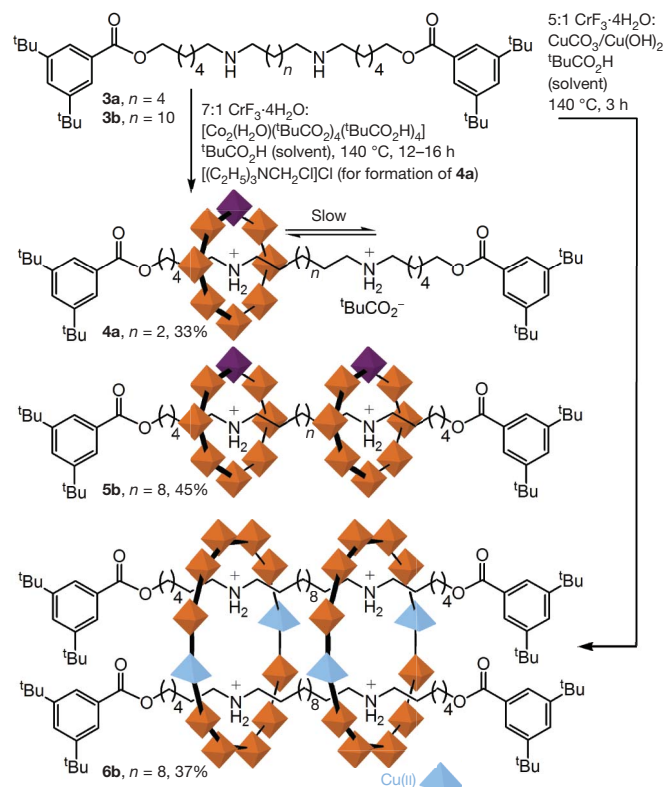


Figure 3 | Synthesis of hybrid organic–inorganic [3]rotaxane 5b, [4]rotaxane 6b and molecular shuttle 4a. Compound 5b has two rings on one thread, 6b has two rings each circumscribing two threads and 4a is a [2]rotaxane in which the ring moves randomly between the two ammonium sites on the thread, restricted by the tight ion-pairing and intercomponent $\text{NH}\cdots\text{F}$ hydrogen-bonding.

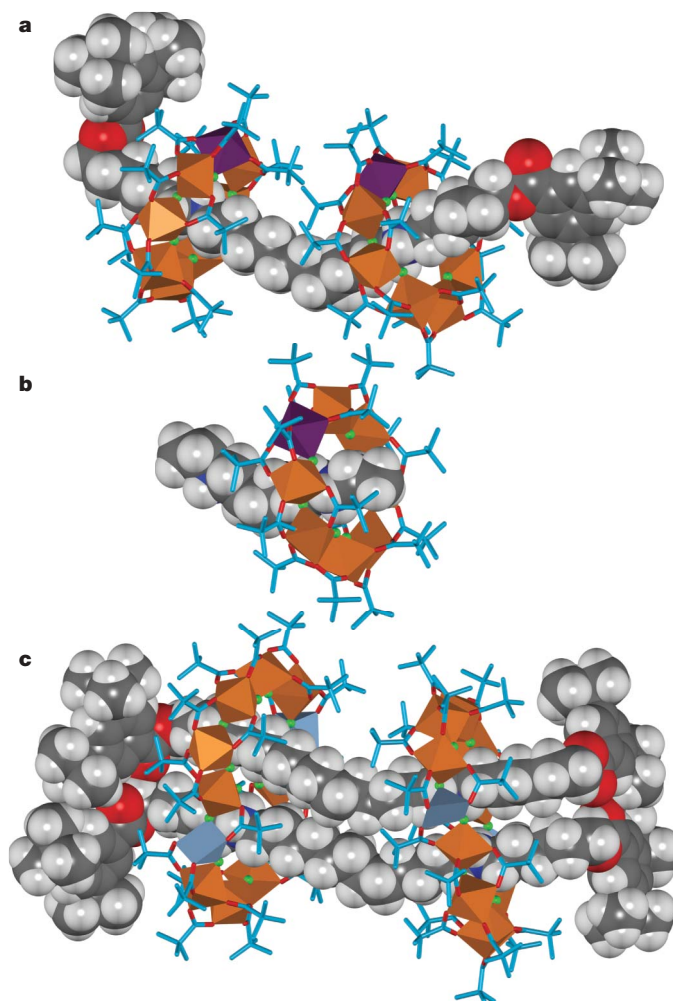


Figure 4 | X-ray crystal structures. a, [3]rotaxane 5b. b, A pseudorotaxane featuring the bisammonium binding-site arrangement present in molecular shuttle 4a. c, [4]rotaxane 6b. The atom representations are as indicated in the legend of Fig. 1b, except that here the organic threads are shown at van der Waals radii and the metal ions of the macrocycles are depicted by solid polyhedra reflecting their coordination geometries: Cr(III), orange octahedron; Co(II), purple octahedron; Cu(II), blue square pyramid. Details of each set of intercomponent binding motifs are provided in the Supplementary Information. In a and b the divalent metal ion, Co(II), is disordered over the eight metal sites on each heterometallic wheel (as for [2]rotaxane 2c; Fig. 1b); in c the divalent metal ion, Cu(II), is localized at the positions indicated. The crystallographic data and experimental details of the structural refinement for 4a, 5b and 6b are provided in the Supplementary Information.

65 components), without any significant quantity (<1%) of the corresponding [2]rotaxane. The X-ray structure (Fig. 4a) of a single crystal of 5b grown from a saturated solution in tetrahydrofuran/acetonitrile shows types of intercomponent interactions similar to those observed with [2]rotaxane 2c, although at one of the macrocycle–thread binding sites the four $\text{NH}\cdots\text{F}$ contacts are of such similar lengths that they can be considered to be pairs of bifurcated $\text{F}^-\cdots\text{H}(\text{N}^+\text{H})\cdots\text{F}^-$ hydrogen bonds (Supplementary Information).

Notably, changing the divalent metal from Co(II) to Cu(II) led to a [4]rotaxane, 6b, with two thread molecules circumscribed by two heterometallic macrocycles²⁸, each ring containing ten octahedral Cr(III) ions and two square-pyramidal Cu(II) ions. By modifying the ratio of the trivalent:divalent metal-salt reagents from 7:1 to the 5:1 required for the stoichiometry of this product, we isolated [4]rotaxane 6b in 37% yield (from 98 components: 24 metal ions, 44 pivalate groups, 28 fluoride ions and two organic threads). The X-ray structure (Fig. 4c) of a single crystal of 6b grown from a saturated

solution of the [4]rotaxane in diethyl ether and acetonitrile was solved with data collected using the Advanced Light Source synchrotron, Lawrence Berkeley National Laboratory. The different coordination requirements of Cu(II) (five coordinate) compared with Co(II) (six coordinate) leads to some enforced changes in the ligand arrangement for the larger heterometallic wheel, and in the [4]rotaxane two of the 14 fluoride ligands are bound to only one metal ion rather than bridging two. These two singly coordinated fluoride anions have a central role as hydrogen-bond acceptors in the intercomponent binding motifs of the [4]rotaxane in the solid state, each being involved in bifurcated hydrogen-bonding to two ammonium groups on different threads (Supplementary Information).

By shortening the spacer between the ammonium units on the thread from twelve (**3b**) to six methylene groups (**3a**)—which is too short to allow heterometallic rings to reside simultaneously on both ammonium sites—and adding (chloromethyl)triethylammonium chloride to the reaction, we were able to form a [2]rotaxane with one heterometallic ring on a thread with two ammonium groups, **4a**, in 33% yield (Fig. 3). The (chloromethyl)triethylammonium chloride was originally introduced accidentally to the reaction as an impurity, produced by the alkylation of triethylamine by dichloromethane during isolation of the thread by column chromatography. However, when subsequent reactions using pure samples of the thread failed to produce any of rotaxane **4a**, analysis of the original procedure established the presence of (chloromethyl)triethylammonium chloride in the successful rotaxane-forming experiment. When (chloromethyl)triethylammonium chloride was deliberately added to the pure thread, the reaction once again produced rotaxane **4a**. Other tetraalkylammonium salts, such as tetraethylammonium chloride, did not promote rotaxane formation when added to the reaction mixture. This suggests that the chloromethyl group has a crucial role, possibly as an electrophilic site of temporary attachment for the tetraalkylammonium cation, which might then act as a macrocyclization template for a growing oligomeric metal-pivalate-fluoride chain.

Unusually for a hydrogen-bonded molecular shuttle, the random back-and-forth shuttling of the macrocycle between the two binding sites on the thread in **4a** occurs on a very different timescale from the spinning of the ring about the axis of the thread. At 300 K, the 500-MHz ^1H NMR spectrum of **4a** in a range of solvents (CDCl_3 , $\text{C}_2\text{D}_2\text{Cl}_4$, d_8 -tetrahydrofuran) shows a well-resolved pair of signals for each chemically distinct 'stopper' proton (Supplementary Information), the difference within each pair being caused by whether the adjacent ammonium centre is vacant or occupied by the heterocyclic ring, indicating that the shuttling between them is slow on the NMR timescale. Heating to 360 K ($\text{C}_2\text{D}_2\text{Cl}_4$ as solvent) did not significantly broaden, let alone coalesce, the signal pairs. However, the dynamic exchange of the ring between the two thread ammonium sites could be measured by polarization transfer between signal pairs during the mixing time in two-dimensional exchange spectroscopy experiments²⁹ (Supplementary Information). These measurements gave a rate of exchange of $1.2 \pm 0.5 \text{ s}^{-1}$ at 330 K in $\text{C}_2\text{D}_2\text{Cl}_4$, corresponding to a free energy of activation (ΔG^\ddagger) for shuttling of $19.3 \pm 0.2 \text{ kcal mol}^{-1}$. This value is at least (and possibly much more than) 10 kcal mol^{-1} higher than the activation barrier to spinning of the ring.

This significant difference can be rationalized from the intercomponent $\text{NH}\cdots\text{F}$ hydrogen-bonding seen in the various crystal structures (Figs 1b and 4). During spinning, the pseudo- C_8 -symmetry of the bridging fluoride ions in the wheel enables the $\text{NH}\cdots\text{F}$ hydrogen bonds to be transferred from one fluoride ion to the next by a low-energy route that does not require significant breaking of an existing hydrogen bond before a new one starts to form, that is, conversion from a 'short' $\text{NH}\cdots\text{F}$ hydrogen bond to a 'long' one through a bifurcated system. These motifs are all seen in the X-ray structures of the various rotaxanes. By contrast, any shuttling mechanism for **4a** must require complete breaking of all the intercomponent $\text{NH}\cdots\text{F}$

hydrogen bonds before translocation of the wheel to the other ammonium binding site can occur.

The linking of organic and inorganic components at the molecular level by mechanical bonding imparts features of both chemistries (for example dynamics and magnetism) to the overall structure, and introduces new and intriguing behaviour through the combination of the two (for example the differences in the mechanisms of rotational and translational intercomponent motion, new non-covalent binding motifs, extreme temperature sensitivity of chemical shifts, novel types of template mechanism and so on). The provision of a simple and versatile synthetic route for linking inorganic and organic components by mechanical bonds at the molecular level should make it possible to create molecules with composite properties, including new behaviours and characteristics that may arise by combining features that have previously been solely the preserve of one type of chemistry or the other.

Received 16 November 2008; accepted 29 January 2009.

1. Yaghi, O. M. *et al.* Reticular synthesis and the design of new materials. *Nature* **423**, 705–714 (2003).
2. Cheetham, A. K. & Rao, C. N. R. There's room in the middle. *Science* **318**, 58–59 (2007).
3. Kitagawa, S., Kitaura, R. & Noro, S.-i. Functional porous coordination polymers. *Angew. Chem. Int. Edn* **43**, 2334–2375 (2004).
4. Ogino, H. Relatively high-yield syntheses of rotaxanes. Syntheses and properties of compounds consisting of cyclodextrins threaded by α , ω -diaminoalkanes coordinated to cobalt(III) complexes. *J. Am. Chem. Soc.* **103**, 1303–1304 (1981).
5. Batten, S. R. & Robson, R. Interpenetrating nets: ordered, periodic entanglement. *Angew. Chem. Int. Edn* **37**, 1460–1494 (1998).
6. Sauvage, J.-P. & Dietrich-Buchecker, C. (eds). *Molecular Catenanes, Rotaxanes and Knots: A Journey through the World of Molecular Topology* (Wiley-VCH, 1999).
7. Loeb, S. J. Metal organic rotaxane frameworks. *Chem. Commun.* 1511–1518 (2005).
8. Fujita, M., Ibukuro, F., Hagihara, H. & Ogura, K. Quantitative self-assembly of a [2]catenane from two preformed molecular rings. *Nature* **367**, 720–723 (1994).
9. Alam, M. A. *et al.* Directed 1D assembly of a ring-shaped inorganic nanocluster templated by an organic rigid-rod molecule. *Angew. Chem. Int. Edn* **47**, 2070–2073 (2008).
10. Anelli, P. L., Spencer, N. & Stoddart, J. F. A molecular shuttle. *J. Am. Chem. Soc.* **113**, 5131–5133 (1991).
11. Berná, J. *et al.* Macroscopic transport by synthetic molecular machines. *Nature Mater.* **4**, 704–710 (2005).
12. Nguyen, T. *et al.* A reversible molecular valve. *Proc. Natl Acad. Sci. USA* **102**, 10029–10034 (2005).
13. Liu, Y. *et al.* Linear artificial molecular muscles. *J. Am. Chem. Soc.* **127**, 9745–9759 (2005).
14. Green, J. E. *et al.* A 160-kilobit molecular electronic memory patterned at 10^{11} bits per square centimetre. *Nature* **445**, 414–417 (2007).
15. Kay, E. R., Leigh, D. A. & Zerbetto, F. Synthetic molecular motors and mechanical machines. *Angew. Chem. Int. Edn* **46**, 72–191 (2007).
16. Leuenberger, M. N. & Loss, D. Quantum computing in molecular magnets. *Nature* **410**, 789–793 (2001).
17. Bertina, S. *et al.* Quantum oscillations in a molecular magnet. *Nature* **453**, 203–206 (2008).
18. Winpenny, R. E. P. Quantum information processing using molecular nanomagnets as qubits. *Angew. Chem. Int. Edn* **47**, 7992–7994 (2008).
19. Larsen, F. K. *et al.* Synthesis and characterization of heterometallic $\{\text{Cr}_7\text{M}\}$ wheels. *Angew. Chem. Int. Edn* **42**, 101–105 (2003).
20. Affronte, M., Carretta, S., Timco, G. A. & Winpenny, R. E. P. A ring cycle: studies of heterometallic wheels. *Chem. Commun.* 1789–1797 (2007).
21. Timco, G. A. *et al.* Influencing the nuclearity and constitution of heterometallic rings via templates. *Chem. Commun.* 3649–3651 (2005).
22. Cador, O. *et al.* The magnetic Möbius strip: synthesis, structure and magnetic studies of odd-numbered antiferromagnetically coupled wheels. *Angew. Chem. Int. Edn* **43**, 5196–5200 (2004).
23. Kolchinski, A. G., Busch, D. H. & Alcock, N. W. Gaining control over molecular threading: benefits of second coordination sites and aqueous–organic interfaces in rotaxane synthesis. *J. Chem. Soc. Chem. Commun.* 1289–1291 (1995).
24. Ashton, P. R. *et al.* Self-assembling [2]- and [3]rotaxanes from secondary dialkylammonium salts and crown ethers. *Chem. Eur. J.* **2**, 729–736 (1996).
25. Mock, W. L., Irra, T. A., Wepsiec, J. P. & Adhia, M. Catalysis by cucurbituril. The significance of bound-substrate destabilization for induced triazole formation. *J. Org. Chem.* **54**, 5302–5308 (1989).
26. Kim, K. Mechanically interlocked molecules incorporating cucurbituril and their supramolecular assemblies. *Chem. Soc. Rev.* **31**, 96–107 (2002).
27. Aucagne, V., Leigh, D. A., Lock, J. S. & Thomson, A. R. Rotaxanes of cyclic peptides. *J. Am. Chem. Soc.* **128**, 1784–1785 (2006).
28. Ashton, P. R. *et al.* Doubly encircled and double-stranded pseudorotaxanes. *Angew. Chem. Int. Edn Engl.* **34**, 1869–1871 (1995).

29. Perrin, C. L. & Dwyer, T. J. Application of two-dimensional NMR to kinetics of chemical exchange. *Chem. Rev.* **90**, 935–967 (1990).

Supplementary Information is linked to the online version of the paper at www.nature.com/nature.

Acknowledgements We thank J. Bella for the exchange spectroscopy NMR experiments, W. Sun for assistance with the preparation of thread **1c** and the Engineering and Physical Sciences Research Council (EPSRC) National Mass Spectrometry Service Centre (Swansea, UK) for high-resolution mass spectrometry. This research was funded by the European Commission (through the NoE 'MAGMANet') and EPSRC. The Advanced Light Source is supported by the Director, Office of Science, Office of Basic Energy Sciences, of the US Department of Energy under contract no. DE-AC02-05CH11231. D.S. is a Swiss National Science Foundation postdoctoral fellow. D.A.L. is an EPSRC Senior Research Fellow and holds a Royal Society Wolfson Research Merit Award.

Author Contributions C.-F.L., D.S. and G.A.T. carried out the synthesis and characterization studies, helped plan the experiments and participated in the preparation of the manuscript. R.G.P. and S.J.T. collected the X-ray data and solved the crystal structures. D.A.L. and R.E.P.W. helped plan the experiments and prepare the manuscript.

Author Information The crystallographic data and experimental details of the structural refinement for the X-ray crystal structures reported in this paper have been deposited at the Cambridge Crystallographic Data Centre, under deposition numbers CCDC 705132–CCDC 705135. These data can be obtained free of charge from the Cambridge Crystallographic Data Centre (http://www.ccdc.cam.ac.uk/data_request/cif). Reprints and permissions information is available at www.nature.com/reprints. Correspondence and requests for materials should be addressed to D.A.L. (david.leigh@ed.ac.uk) or R.E.P.W. (richard.winpenny@manchester.ac.uk).